JOURNAL OF VIROLOGY, July 2009, p. 7029–7039 Vol. 83, No. 14
0022-538X/09/$08.00+0 doi:10.1128/JVI.00329-09

The RING Domain and the L79 Residue of Z Protein Are Involved in both the Rescue of Nucleocapsids and the Incorporation of Glycoproteins into Infectious Chimeric Arenavirus-Like Particles[▽]

Juan Cruz Casabona,[1] Jesica M. Levingston Macleod,[1] Maria Eugenia Loureiro,[1] Guillermo A. Gomez,[2] and Nora Lopez[1]*

Centro de Virología Animal (CEVAN), Instituto de Ciencia y Tecnología Dr. Cesar Milstein, Consejo Nacional de Ciencia y Tecnología (CONICET), Saladillo 2468, C1440FFX Ciudad Autónoma de Buenos Aires, Argentina,[1] and Centro de Investigaciones en Química Biológica de Córdoba (CIQUIBIC, UNC-CONICET), Departamento de Química Biológica, Facultad de Ciencias Químicas, Universidad Nacional de Córdoba, Córdoba X5000HUA, Argentina[2]

Received 13 February 2009/Accepted 24 April 2009

Arenaviruses, such as Tacaribe virus (TacV) and its closely related pathogenic Junin virus (JunV), are enveloped viruses with a bipartite negative-sense RNA genome that encodes the nucleocapsid protein (N), the precursor of the envelope glycoprotein complex (GP), the polymerase (L), and a RING finger protein (Z), which is the driving force of arenavirus budding. We have established a plasmid-based system which allowed the successful packaging of TacV-like nucleocapsids along with Z and GP of JunV into infectious virus-like particles (VLPs). By coexpressing different combinations of the system components, followed by biochemical analysis of the VLPs, the requirements for the assembly of both N and GP into particles were defined. We found that coexpression of N with Z protein in the absence of minigenome and other viral proteins was sufficient to recruit N within lipid-enveloped Z-containing VLPs. In addition, whereas GP was not required for the incorporation of N, coexpression of N substantially enhanced the ratio of GP to Z into VLPs. Disruption of the RING structure or mutation of residue L79 to alanine within Z protein, although it had no effect on Z self-budding, severely impaired VLP infectivity. These mutations drastically altered intracellular Z-N interactions and the incorporation of both N and GP into VLPs. Our results support the conclusion that the interaction between Z and N is required for assembly of both the nucleocapsids and the glycoproteins into infectious arenavirus budding particles.

The family *Arenaviridae* currently comprises at least 22 species of largely rodent-borne viruses that can be divided into Old and New World complexes (4, 7). The Old World complex includes the human pathogens lymphocytic choriomeningitis virus (LCMV) and Lassa fever virus (LFV). Within the New World group, the viruses can be classified into three phylogenetically distinct clades. One of those clades includes Tacaribe virus (TacV), the prototype of the New World complex, and the known South American pathogens that produce severe hemorrhagic disease in humans: Junin (JunV), Machupo, Guanarito, and Sabia viruses (4, 7). JunV is the etiological agent of Argentine hemorrhagic fever and has been recognized as a serious public health problem (13). Despite its close relationship with the pathogenic JunV and Machupo virus, TacV has not been associated with human illness (7, 28).

Arenaviruses are enveloped viruses whose genomes consist of two single-stranded, negative-sense RNA segments named S (ca. 3.4 kb) and L (ca. 7.2 kb). The S RNA contains two genes encoding the nucleoprotein (N; ca. 64 kDa) and the glycoprotein precursor (GPC; ca. 70 kDa) (5). Posttranslational proteolytic processing of GPC yields three noncovalently associated subunits which form the envelope glycoprotein complex (GP): the peripheral receptor-binding (G1) and the transmembrane (G2) proteins and a stable signal peptide (5). The L RNA encodes the RNA-dependent RNA polymerase (L protein; ca. 200 kDa) and a protein with a RING finger motif (Z; ca. 11 kDa), which exhibits an inhibitory effect on viral RNA replication and transcription (8, 9, 27) through its interaction with the L protein (21, 48). In both S and L RNAs, the genes are arranged in opposite orientation and are separated by a noncoding intergenic region. Genomes and antigenomes are found tightly bound to the N protein forming nucleocapsids, which are the functional templates for transcription and replication (2, 16, 41).

Several lines of evidence indicate that Z protein, in addition to its role as a potent inhibitor of virus RNA synthesis, is involved in arenavirus assembly and budding from the plasma membrane. Specifically, LCMV and LFV Z proteins, which contain PTAP and/or PPPY late domains that are necessary for efficient budding, are able by themselves to direct the budding of lipid-enveloped virus-like particles (VLPs) from the cell surface (37, 46). Late domains in matrix proteins of many other enveloped RNA viruses mediate the recruitment of cellular proteins that assist in the late stages of budding (31, 44). Accordingly, both LFV and LCMV Z proteins use cellular proteins of the multivesicular body pathway in budding (37,

* Corresponding author. Mailing address: Centro de Virología Animal, Instituto de Ciencia y Tecnología Dr. Cesar Milstein, CONICET, Saladillo 2468, C1440FFX Ciudad Autónoma de Buenos Aires, Argentina. Phone and fax: 54 11 46876735. E-mail: nlopezcevan@centromilstein.org.ar.

▽ Published ahead of print on 6 May 2009.

47). In addition, like other viral matrix proteins, LCMV and LFV Z proteins are associated with the plasma membrane (37, 46). Indeed, cryoelectron microscopy analysis supports a membrane-proximal location of Z within arenavirus virions (33).

On the basis of observations indicating that Z and N proteins in purified LCMV form a complex after chemical crosslinking (42) and that Z and N proteins of LFV interact in vivo, it has been suggested that the interaction between Z and N might be implicated in the recruitment of nucleocapsids to cellular membranes during virus maturation (12). In this report, we studied the molecular determinants that are involved in Z-N interactions and their role in arenavirus assembly and budding. To this end, we established a plasmid-based system that allows the encapsidation, replication, and packaging of a synthetic TacV S genome analog (minigenome) into infectious VLPs. Using this system, we demonstrated that Z protein is necessary and sufficient to recruit N protein into Z-induced particles that are surrounded by a lipid envelope and showed that the RING structure and residue L79 of Z are required for intracellular Z-N interactions and are critically important for the recruitment of both N and GP into infectious particles.

MATERIALS AND METHODS

Cells and virus. BSR (a clone of BHK-21) cells and CV1 cells were grown in a 5% CO_2 atmosphere at 37°C by using Glasgow minimum essential medium (Invitrogen) and Dulbecco's modified Eagle's medium (Invitrogen), respectively. Growth medium was supplemented with 10% fetal calf serum (FCS; Invitrogen) and penicillin (100 U/ml)-streptomycin (100 μg/ml) (Invitrogen). Recombinant vaccinia virus vTF7-3, which expresses the T7 RNA polymerase (18), was kindly provided by Bernard Moss (National Institutes of Health, Bethesda, MD).

Plasmids. Plasmid pS-CAT expresses a TacV S RNA analog consisting of the entire S genome 5′ untranslated region (UTR) sequence, followed by 171 nucleotides of the 3′ terminal region of the GPC open reading frame (ORF) plus the complete S intergenic sequence, then the chloramphenicol acetyltransferase (CAT) ORF in an antisense orientation, and the complete S genome 3′ UTR sequence. Plasmid pS-CAT was generated by PCR amplification using plasmid pWT (26) as a template. The forward primer included (5′ to 3′) a sequence comprising a BbsI site, followed by a G residue to provide for a 5′ extra G in the genomic transcript (as reported for the 5′ termini of arenavirus genomic and antigenomic RNAs [23]), and then a sequence corresponding to positions 1 to 19 of the TacV S genomic 5′ UTR. The reverse primer comprised (5′ to 3′) a BbsI site followed by a sequence complementary to positions 3422 to 3397 of the TacV S genome (numbers indicate positions relative to the 5′ end of the S genome-sense sequence). The purified PCR amplification product was digested with BbsI and then inserted between the BbsI sites of plasmid pRF42, provided by Ramon Flick (University of Texas, Galveston, TX). The location of the expression cassette between the murine RNA polymerase I promoter and terminator allows the generation of a transcript with no additional nucleotides at the 5′ and 3′ termini (15). The ORFs corresponding to TacV Z, TacV N, TacV L, TacV GPC, and JunV GPC were obtained from previously described constructs (25, 27), either by digestion with the appropriate restriction enzymes or by PCR amplification, and then cloned between the NcoI and SmaI sites of pTM1 vector (a gift of B. Moss), yielding plasmids pTacV Z, pTacV N, pTacV L, pTacV GP, and pJunV GP, respectively. The JunV Z ORF was amplified by reverse transcription-PCR using total RNA extracted from JunV XJ strain-infected Vero cells (obtained from Elsa Damonte, University of Buenos Aires, Argentina) and primers designed on the basis of reported JunV sequences (GenBank accession number AY358022), such that an NcoI site at the AUG and a SmaI site after the stop codon were introduced. After digestion with NcoI and SmaI, the PCR product was cloned between the same sites of pTM1, generating plasmid pJunV Z. To allow their detection, both JunV Z and TacV Z proteins were joined at their C termini with a sequence comprising an influenza hemagglutinin (HA) epitope (GSYPYDVPDYA). To this aim, both HA-tagged ORFs were obtained by PCR using either pJunV Z or pTacV Z as a template and then cloned between the NcoI and SacI sites of pTM1, generating plasmids pJunV Z-HA and pTacV Z-HA, respectively. Transfection of parallel cell cultures with comparable amounts of pJunV Z-HA and pTacV Z-HA leads to similar Z protein expression levels, as determined by Western blotting (data not shown). To construct TacV N protein tagged at its N terminus with either the Flag epitope (DYKDDDDK) or a c-Myc epitope (MAEQKLISEEDL), pTacV N was used as a template to amplify the corresponding PCR fragments, which were purified, digested with NcoI and SmaI, and then cloned between the NcoI and SmaI sites of pTM1 vector, obtaining plasmids pTacV N-Flag and pTacV N-myc, respectively. Both N-Flag and N-myc proteins supported infectious VLP production at levels similar to those of untagged N protein, indicating that the tags did not interfere with the functions of N (not shown).

Mutations in the JunV Z ORF were introduced by using a QuickChange PCR mutagenesis kit (Stratagene) with primers containing the mutated sequences and plasmid pJunV Z-HA as a template. All constructs were checked by dideoxynucleotide double-strand DNA sequencing (Macrogen Inc.). All primer sequences and vector maps are available upon request. Plasmid pCMV-T7pol expresses the bacteriophage T7 RNA polymerase under the control of the cytomegalovirus promoter (38) and was kindly provided by Martin A. Billeter (University of Zurich, Irchel, Switzerland).

DNA transfections, VLP generation and purification, and infectivity assay. BSR cells grown in 12-well plates were transfected using Lipofectamine 2000 reagent (Invitrogen) according to the manufacturer's instructions. For VLP generation, the transfection medium was removed after 4 h of incubation, cells were washed twice, fresh medium supplemented with 2% FCS was added, and the incubation was continued. For the infectivity assay, the transfected cell monolayers were collected at 72 h posttransfection and analyzed for reporter CAT expression (Fig. 1, Transfection; see also Fig. 4). The corresponding supernatants were clarified by low-speed centrifugation (4,000 × *g* for 10 min at 4°C) and transferred to CV1 cells grown in 12-well plates. After 2 h of adsorption, the inoculum was removed, and cells were washed with fresh medium and subsequently transfected with 1 μg each of pCMV-T7pol, pTacV N, and pTacV L per well. The transfection medium was replaced by fresh medium (2% FCS) at 4 h posttransfection, and 48 h later cells were analyzed for CAT expression (Fig. 1, Passage; see also Fig. 4). CV1 cells were chosen for these assays because this cell line is susceptible to TacV and JunV infections (25) and also because higher levels of CAT activity passage were achieved than in VLP-infected BSR cells (data not shown). The amounts of plasmid DNA used for complete VLP production were the following: 1 μg of pCMV-T7pol, 3 μg of pS-CAT, 3 μg of pTacV N, 1 μg of pTacV L, 0.15 to 0.3 μg of either pTacV Z-HA or pJunV Z-HA, and 2 μg of either pTacV GP or pJunV GP, per well, as determined under our experimental conditions (data not shown). All other transfections, with the exception of those performed for coimmunoprecipitation assays (see Fig. 5C), also included 1 μg of pCMV-T7pol per well in addition to the indicated plasmids. In all transfections, the total amount of transfected DNA was kept constant by the addition of vector pTM1 DNA. All plasmids were purified by Qiagen tip-100 (Qiagen Inc.).

For VLP purification, the supernatants from transfected cells were collected, clarified by centrifugation as described above, layered over 20% (wt/vol) sucrose cushions in TNE buffer (50 mM Tris-HCl [pH 7.4], 150 mM NaCl, 1 mM EDTA), and then centrifuged at 34,000 rpm for 2 h at 4°C in a Beckman SW 50.1 rotor. The pelleted VLPs were resuspended and analyzed as indicated below.

Metabolic labeling and immunoprecipitation. Transfected BSR cell monolayers were washed twice at 16 h posttransfection and then metabolically labeled by the addition of [^{35}S]methionine-cysteine mix (150 μCi/ml; NEN Perkin Elmer) in cysteine-methionine-free medium supplemented with 2% FCS. Following 7 h of labeling, supernatants were saved, and the incubation of the monolayer was continued with regular growth medium. After an additional 16-h incubation, the medium was harvested and pooled with the corresponding previously collected supernatant, and VLPs were purified as indicated above. Labeled VLPs were resuspended in radioimmunoprecipitation assay buffer (50 mM Tris [pH 7.5], 150 mM NaCl, 1.0%, NP-40, 0.5% sodium deoxycholate, 0.1% sodium dodecyl sulfate), supplemented with protease inhibitors (2 μg/ml aprotinin, 20 μg/ml phenylmethylsulfonyl fluoride, 50 μg/ml *N*-α-tosyl-L-lysine chloromethyl ketone [Sigma-Aldrich]). Cell monolayers were washed twice with 1× phosphate-buffered saline (PBS) and then lysed by the addition of TNE-N (0.2% Nonidet P-40 in TNE buffer) containing protease inhibitors. Cell lysates were clarified at 16,000 × *g* for 20 min at 4°C. Aliquots corresponding to about 1×10^5 to 4×10^5 cells of both cell extracts and VLPs were used for immunoprecipitation with appropriate antibodies, as described previously (21). Antisera used were the following: rabbit anti-TacV N polyclonal serum (40), rabbit anti-HA polyclonal antibody (Santa Cruz Biotechnology), mouse monoclonal antibody (MAb) QC03-BF11 directed against the G1 subunit of JunV GP (43) (obtained through the NIH Biodefense and Emerging Infections Research Resources Repository, National Institute of Allergy and Infectious Diseases, NIH), and mouse anti-Flag M2 MAb (Sigma-Aldrich). Proteins were analyzed by sodium dodecyl sulfate-

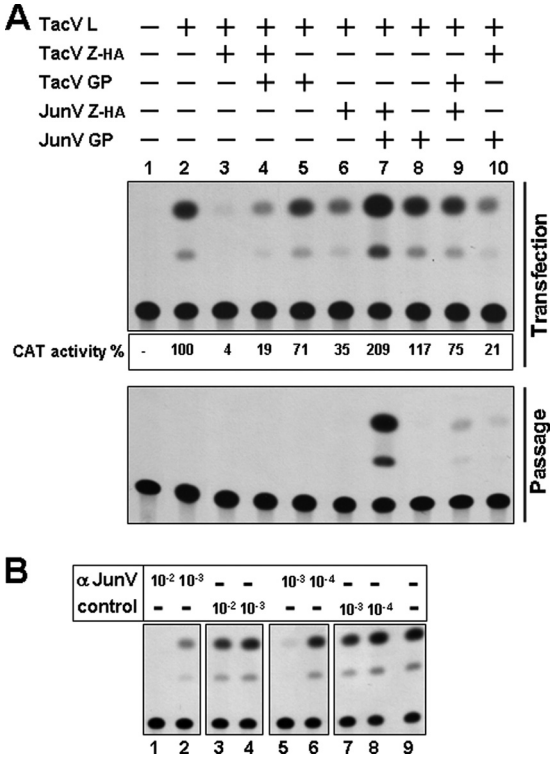

FIG. 1. Generation of infectious VLPs. (A) BSR cells were transfected with plasmids expressing S-CAT minigenome and TacV N, along with the plasmids encoding the proteins indicated at the top of the panel (+) at the amounts indicated in Materials and Methods. At 72 h posttransfection, cell supernatants were harvested, and cell extracts were prepared for determination of CAT activity (Transfection). The supernatants collected from transfected cells were clarified and added to CV1 cell monolayers, which were then assayed for CAT activity (Passage), as indicated in Materials and Methods. CAT activities in transfections were quantified, and the mean values from three independent experiments are presented (CAT activity %) as a percentage of that corresponding to lane 2, taken as 100%. (B) Inhibition of CAT activity passage by incubation with anti-JunV neutralizing antibodies. Equivalent aliquots of clarified culture supernatant collected from cells transfected as in lane 7 in panel A were mixed with the indicated dilutions of a rabbit anti-JunV serum (provided by E. Damonte) (lanes 1 and 2), a control rabbit serum (lanes 3 and 4), anti-JunV G1 QC03-BF11 MAb (43) (lanes 5 and 6), or normal ascites (lanes 7 and 8). Following incubation at 37°C for 60 min, mixes were used to inoculate CV1 cell monolayers, which were then assayed for CAT activity as indicated in Materials and Methods. Reaction products from untreated supernatant-infected cell lysates are shown in lane 9. α, anti.

polyacrylamide gel electrophoresis (SDS-PAGE) on 10% (for N) or 12% (for Z and G1) polyacrylamide gels together with ^{14}C-labeled markers and then visualized by exposure to X-ray films (Kodak), as described before (25). When indicated, quantification of the gels was performed by densitometry using ImageJ software (1).

Western blotting. Transfected BSR cells were lysed at 48 h posttransfection in nonreducing SDS-PAGE sample buffer (Invitrogen). The corresponding culture supernatants were collected, and the VLPs, purified as indicated above, were resuspended in nonreducing SDS-PAGE sample buffer. After addition of 0.1% β-mercaptoethanol, samples were boiled for 5 min, and amounts of cell lysates corresponding to 0.5×10^5 to 1×10^5 cells or amounts of resuspended VLPs corresponding to 1×10^5 to 2×10^5 cells were loaded per lane and fractionated by SDS–12% PAGE. Resolved proteins were transferred to Hybond-ECL nitrocellulose membranes (GE Healthcare), and blots were stained with Ponceau-S (Sigma-Aldrich) before being blocked overnight at 4°C with 5% skim milk in PBS-T (0.1% Tween 20 [Sigma-Aldrich] in PBS). Blots were then incubated with primary antibody for 2 h at 37°C, washed five times with PBS-T, and incubated with secondary antibody for 1 h at room temperature. Next, blots were washed five times with PBS-T, followed by incubation with SuperSignal West Pico chemiluminescent substrate (Thermo Scientific) for detection of horseradish peroxidase, according to the manufacturer's specifications. Finally, blots were exposed to X-ray films, and protein bands were quantified by densitometry as indicated above.

Primary antibodies were the following: rabbit anti-HA polyclonal antibody (Santa Cruz Biotechnology) and mouse anti-Flag M2 MAb (Sigma Aldrich) or rabbit anti-TacV N polyclonal serum (40). Horseradish peroxidase-conjugated anti-mouse or anti-rabbit (Jackson ImmunoResearch) was used as a secondary antibody, according to protocols of the suppliers. For Z self-budding estimation (see Fig. 4D), the amount of Z was normalized to the amount of β-tubulin in cell extracts by probing blots with an anti-β-tubulin MAb (Sigma-Aldrich), followed by enhanced chemiluminescence and densitometry, as described above.

Protease protection assay. Transfection of BSR cells, metabolic labeling, and purification of VLPs were performed as described above. Labeled VLPs were resuspended overnight at 4°C in STE buffer (10 mM Tris-HCl [pH 7.5], 100 mM NaCl, 1 mM EDTA [pH 8.0]). This resuspension was divided into three equal aliquots: aliquot 1 was left untreated, aliquot 2 received trypsin (Sigma-Aldrich) to a final concentration of 0.1 mg/ml, and aliquot 3 was adjusted with Triton X-100 to a final concentration of 1% prior to the addition of trypsin (0.1 mg/ml). Samples were incubated at room temperature for 30 min, and then *N*-α-tosyl-L-lysine chloromethyl ketone (0.25 mg/ml) and aprotinin (0.6 mg/ml) were added to each aliquot. All reaction mixtures were adjusted to a final concentration of 1% of Triton X-100 in STE buffer and then diluted with radioimmunoprecipitation assay buffer prior to immunoprecipitation, as indicated before.

Coimmunoprecipitation analysis. CV1 cells grown in 12-well dishes were infected with 3 to 5 PFU per cell of vaccinia virus vTF7-3 expressing the T7 RNA polymerase (18) and then transfected with (amounts per well) 1 μg of pTacV N-myc together with 1.5 μg of either pJunV Z-HA or each of the mutant Z-expressing plasmids, as indicated in Fig. 5C. Parallel cultures were transfected with either 1.5 μg of pJunV Z-HA or 0.3 μg of pTacV N-myc alone. Transfected cells were metabolically labeled, clarified cell lysates were obtained, and aliquots of the cell extracts corresponding to 1×10^5 to 2×10^5 cells were immunoprecipitated using either anti-HA or anti-c-Myc polyclonal antibody (Santa Cruz Biotechnology), as previously described (21). Labeled immunoprecipitated proteins were resolved by SDS–12% PAGE, visualized by autoradiography, and quantified by densitometry. Z-N binding was estimated as indicated before (21).

CAT activity assay. CAT activity was assayed in extracts from transfected BSR cells or from VLP-infected CV1 cells, as described before (27). CAT activity was calculated by determining the percentage of radioactivity associated with monoacetylated chloramphenicol species relative to total radioactivity. Quantification was performed as previously described (27).

Immunofluorescence and confocal microscopy. BSR cells grown on glass coverslips within 12-well dishes were transfected with 0.5 μg per well of either pTacV N, pJunV Z-HA, or each of the mutant Z-expressing plasmids; alternatively, cells were transfected pairwise with 0.5 μg of each plasmid, as indicated in the legend for Fig. 5B. At 24 h posttransfection, cells were washed twice with 1× PBS and fixed with 4% paraformaldehyde for 10 min at room temperature. After cells were washed with PBS, they were permeabilized using 0.2% Triton X-100 for 10 min at room temperature, blocked with PBS containing 3% bovine serum albumin (BSA) for 1 h, and incubated with a mix of primary antibodies for 1 h at 37°C. Cells were then washed extensively in PBS–3% BSA and incubated with a mix of secondary antibodies for 1 h at 37°C. After the cells were washed, they were mounted on FluorSave (Calbiochem). Confocal images were collected with a Carl Zeiss LSM5 Pascal laser scanning confocal microscope (Carl Zeiss), using a 63× (1.4 numerical aperture) Plan-Apochromat oil immersion objective (Carl Zeiss) or a 100× UPlanSApo oil immersion objective (1.4 numerical aperture; Olympus) with an appropriate pinhole to obtain 1 Airy unit (optical slice, 0.8 μm). Emission filters set for fluorescein and rhodamine were previously described (20).

The primary antibody mixture consisted of rabbit anti-HA polyclonal antibody (Santa Cruz Biotechnology) and mouse anti-TacV N (2.52.2) MAb (19) (kindly provided by Michael Buchmeier, The Scripps Research Institute, La Jolla, CA) in PBS containing 3% BSA. The secondary antibody mixture contained Alexa Fluor 488 chicken anti-mouse immunoglobulin G (Invitrogen) to detect N protein and Alexa Fluor 568 goat anti-rabbit immunoglobulin G (Invitrogen) to detect the HA-tagged Z proteins.

RESULTS

Generation of infectious VLPs. By using a reverse genetic approach, we have previously demonstrated that TacV L and N are the only viral proteins required for full-cycle RNA replication and transcription and that Z protein is a powerful inhibitor of these processes (27). We now use reverse genetics to study the mechanisms regulating TacV morphogenesis. To develop a system reproducing the complete virus life cycle, genes encoding TacV proteins were cloned downstream of the T7 promoter and the internal ribosome entry site of encephalomyocarditis virus into the cap-independent pTM1 expression vector (32). The expression of plasmids encoding viral proteins was driven by the T7 RNA polymerase supplied upon cotransfection with plasmid pCMV-T7pol (38). A synthetic minigenome, designated S-CAT, encoding a CAT reporter gene flanked by the TacV S-genome noncoding sequences, was expressed under the control of the RNA polymerase I from the plasmid pS-CAT (Materials and Methods). The amounts of plasmids encoding TacV N and L proteins used in the transfections were optimized along with the amount for the S-CAT minigenome to maximize CAT expression in transfected cells (data not shown). To generate VLPs, we included a tagged version of TacV Z (TacV Z-HA), carrying an influenza HA epitope at its C terminus (Materials and Methods) as it has been demonstrated that C-terminal tags do not interfere with the functions of Z protein (37). Consistent with our previous findings (27), coexpression of TacV Z-HA protein together with N and L reduces the levels of CAT activity to about 4% of that exhibited by cells expressing N and L alone (Fig. 1A, Transfection, compare lanes 2 and 3). Expression of TacV GP in the absence of Z had almost no effect on CAT activity relative to the control (lane 5), whereas coexpression of both TacV GP and TacV Z-HA with N and L proteins slightly diminished the inhibitory effect of Z protein from about 95% to near 80% (compare lanes 3 and 4). To evaluate whether infectious VLPs were generated, aliquots of the culture medium from these cells were then used to inoculate CV1 cells that were subsequently transfected with N- and L-expressing plasmids to support transcription and replication of the eventually transferred minigenome. The successful assembly of the minigenome into the VLPs and its transfer through infection were monitored by measuring CAT activity (Fig. 1A, Passage). No CAT activity was transferred by the supernatants from cells coexpressing all four TacV proteins (lane 4) or by those from cells coexpressing N and L proteins with either Z-HA or GP (lanes 3 and 5). Consistently, undetectable levels of CAT passage were obtained by using either different amounts of TacV Z- and/or GP-expressing plasmids or the untagged version of TacV Z in transfection. Further, these results were reproduced by using either BSR or BHK-21 cells for passage (data not shown).

A possible explanation for the failure of TacV Z and GP to mediate detectable infectious VLP formation could be related to the low levels of minigenome replication observed in VLP producer cells (Fig. 1A, Transfection lane 4). As preliminary experiments revealed that JunV Z fused at its C terminus to an HA epitope (JunV Z-HA [Materials and Methods]) displayed a lower inhibitory effect on S-CAT minigenome synthesis than comparable amounts of TacV Z-HA, we exchanged TacV Z-HA with JunV Z-HA in the system (Fig. 1A, lanes 6, 7, and 9). Quantification of the results showed that JunV Z-HA exhibits an inhibitory effect on S-CAT expression nearly 10-fold lower than that of TacV Z-HA (Transfection, compare lanes 3 and 6). Further, coexpression of both JunV GP and JunV Z-HA together with the support N and L proteins raised CAT activity to levels twofold higher than those achieved when GP and Z were omitted (Transfection, compare lane 7 with lane 2), and when the supernatants from these cells were used to inoculate CV1 cells, high levels of CAT activity passage were detected (Fig. 1A, Passage, lane 7), whereas no CAT activity could be transferred when plasmids expressing either JunV Z-HA or JunV GP were omitted (lanes 8 and 6). However, almost undetectable levels of reporter gene transfer were observed upon coexpression of support proteins together with either JunV Z and TacV GP or TacV Z and JunV GP (Passage, lanes 9 and 10). Similar results were obtained by using the untagged version of JunV Z or when BHK-21 cells were used for VLP production and/or to perform the VLP infectivity assays (not shown), confirming that TacV-like nucleocapsids can be successfully packaged into infectious VLPs together with JunV Z and JunV GP. We then adopted this combination of proteins for further experiments.

To evaluate the ability of the system to produce VLPs able to initiate infection in the same manner as authentic JunV, we examined whether JunV-neutralizing antibodies could inhibit VLP infection and the consequent passage of CAT activity to new cells (Fig. 1B). Results showed that the transmission of CAT activity was inhibited upon incubation of supernatants from cells expressing TacV N, TacV L, JunV Z, and JunV GP, with either anti-JunV polyclonal serum (lanes 1 and 2) or a JunV G1-directed MAb (lanes 5 and 6). The same dilutions of preimmune serum (lanes 3 and 4) or normal mouse ascites (lanes 7 and 8) did not affect infectivity compared to untreated supernatants (lane 9). These results clearly indicated that infection was mediated by the JunV GP, suggesting that the VLP envelope would be similar to that of the standard Junin virions.

Biochemical characterization of VLPs. To investigate the individual contribution of viral proteins to VLP assembly, we characterized the particles released into the culture medium of cells expressing the S-CAT minigenome and TacV L protein along with different combinations of TacV N, JunV GP, and JunV Z-HA proteins. To this end, radioactively labeled VLPs were analyzed by immunoprecipitation with specific sera, followed by gel electrophoresis (Fig. 2, lanes 1 to 4). As a control, aliquots of the VLP-producing cell extracts were also immunoprecipitated (Fig. 2, lanes 5 to 8). Results showed that N as well as G1 and Z proteins were clearly detected when the supernatants from cells coexpressing the complete set of proteins in addition to the S-CAT minigenome were immunoprecipitated using either serum against N or a mixture of anti-G1 and anti-HA antibodies (lane 4). When Z protein was not coexpressed, no N and almost undetectable amounts of G1 were found in the supernatants (lane 3). In addition, the release of Z into the culture medium was not affected by the omission of either pTacV N or pJunV GP from the transfection mixture (Fig. 2, lower panel, lanes 1 and 2). Immunoprecipitation of the supernatants with serum to TacV N revealed that coexpression of N and Z with the S-CAT minigenome and L allowed the release of N (panel α-N, lane 2), indicating that

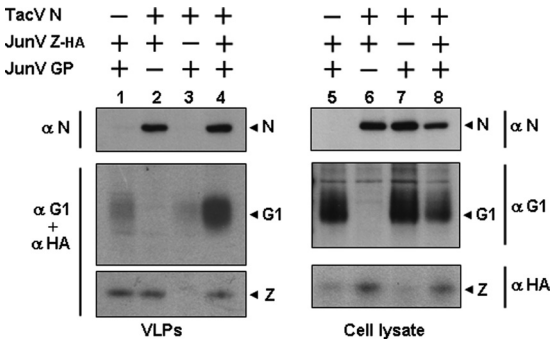

FIG. 2. Immunoprecipitation of VLPs with specific sera. BSR cells were transfected with pS-CAT and pTacV L, together with the plasmids encoding the proteins indicated at the top of the panel (+) at the amounts used to generate complete VLPs (Materials and Methods). Cells were metabolically labeled, and VLPs were prepared as described in Materials and Methods. Aliquots of both cell lysate and VLPs were immunoprecipitated using antibodies against either JunV G1 (α G1), TacV N (α N), the HA epitope (α HA), or a mix of anti-JunV G1 and anti-HA antibodies (α G1+α HA). Precipitated polypeptides were resolved by SDS-PAGE, visualized by autoradiography, and quantified (Materials and Methods). The positions of G1, N, and Z-HA (Z) are indicated by arrowheads. α, anti.

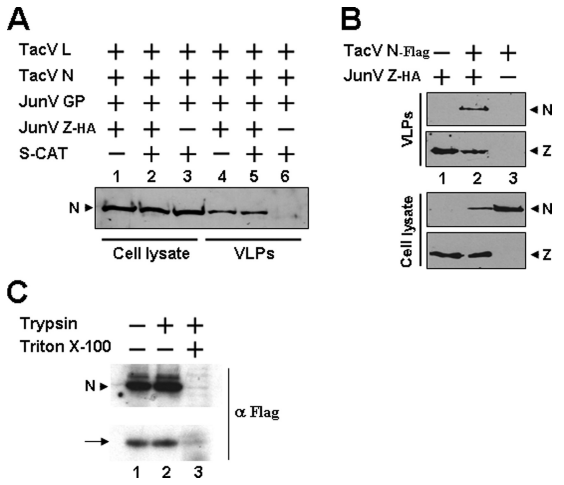

FIG. 3. Recruitment of N into VLPs. (A) BSR cells were transfected with the complete set of plasmids at the amounts indicated in Materials and Methods. When indicated (−), either the S-CAT minigenome- or the JunV Z-HA-expressing plasmid was omitted from the transfection mix. Cell lysates and VLPs were prepared as described in Materials and Methods. Samples of both cell lysates (lanes 1 to 3) and purified VLPs (lanes 4 to 6) were analyzed by SDS-PAGE, followed by immunoblotting using anti-TacV N serum. (B) BSR cells grown in 12-well plates were transfected with 0.5 μg of pJunV Z-HA together with 1 μg of pTacV N-Flag (lane 2). As a control, the same amounts of pJunV Z-HA (lane 1) or pTacV N-Flag (lane 3) were solitarily transfected. Cell lysates and VLPs were prepared as in panel A, and proteins were resolved by SDS-PAGE and analyzed by Western blotting, using specific serum against either TacV N or the HA epitope. (C) Cells grown in 12-well plates were transfected as in lane 2 in panel B and then metabolically labeled as indicated in Materials and Methods. Labeled VLPs, purified from the supernatant of about 1.5×10^6 transfected cells, were resuspended in STE buffer and then divided into three equal aliquots, which were either left untreated (lane 1) or treated with either trypsin (lane 2) or a mix of Triton X-100 and trypsin (lane 3). Labeled proteins were then immunoprecipitated with serum against the Flag epitope (α Flag), resolved by SDS-PAGE, and visualized by autoradiography. Arrowheads in panels A to C indicate the positions of Z-HA (Z) and either N or N-Flag (N).

GP was not required. By contrast, the omission of N caused a severe reduction in the amount of G1 immunoprecipitated from the culture medium compared to that detected in supernatants from cells coexpressing GP along with N and Z (Fig. 2, compare lanes 1 and 4 of panel α G1+α HA). The results from three independent experiments revealed that cells cotransfected with the complete set of plasmids produced VLPs with a ratio of G1 to Z about 5- to 10-fold higher than the ratio observed in VLPs produced in the absence of N. Immunoprecipitation of the cell lysates with specific serum (lanes 5 to 8) showed that the omission of pTacV N from the transfection mixture did not affect the intracellular accumulation or stability of GP (panel α G1, lane 5). Further, control experiments revealed that intracellular levels of Z in cells coexpressing N and GP were similar to those detected in cells in which N was omitted, as determined by Western blotting using anti-HA antibodies (not shown).

Taken together, these results demonstrated that JunV Z is strictly required for the release of N and showed that, whereas GP is not required for the incorporation of N, coexpression of N substantially enhanced the ratio between GP and Z detected in Z-directed VLPs, suggesting a critical role of N in the incorporation of GP into budding particles.

N is recruited into VLPs upon coexpression with Z protein. We then investigated whether the release of TacV N is dependent on the coexpression of S-CAT minigenome. To address this point, BSR cells were transfected with the complete set of plasmids (encoding L, N, Z, GP, and S-CAT RNA) or with a mixture in which either the Z- or the minigenome-expressing plasmid was omitted. Culture supernatants were collected, and VLPs were purified and analyzed by Western blotting (Fig. 3A). Results showed, as expected, that no N protein was detected in the culture medium of transfected cells when the Z-expressing plasmid was omitted from the transfection mix (lane 6) and revealed that cells transfected with the complete VLP-producing system released levels of N as good as those released from cells in which the minigenome was omitted (compare lane 5 with lane 4). Moreover, as seen in Fig. 3B, when Z and N were coexpressed in the absence of other viral proteins or RNA analogs, N was released into the supernatant of transfected cells together with Z (lane 2) while N expressed alone was not released (lane 3), indicating that Z is sufficient to drive the release of N. Control cultures expressing JunV Z alone released Z into the supernatant (lane 1), demonstrating that JunV Z displays an intrinsic budding ability, as previously shown for LCMV and LFV (37, 46). To confirm that N was incorporated into Z-induced VLPs, supernatants from cells coexpressing N and Z were subjected to a protease protection assay, followed by immunoprecipitation of N protein (Materials and Methods). As seen in Fig. 3C, N protein remained largely protected from protease digestion (compare lanes 1 and 2) while the addition of detergent resulted in the complete degradation of N by the protease (lane 3). These results demonstrated that N is incorporated into Z-induced particles that are surrounded by a lipid envelope. Interestingly, results also revealed that a protein comigrating with Z-HA (Fig. 3C, arrow) coimmunoprecipitated together with undegraded N

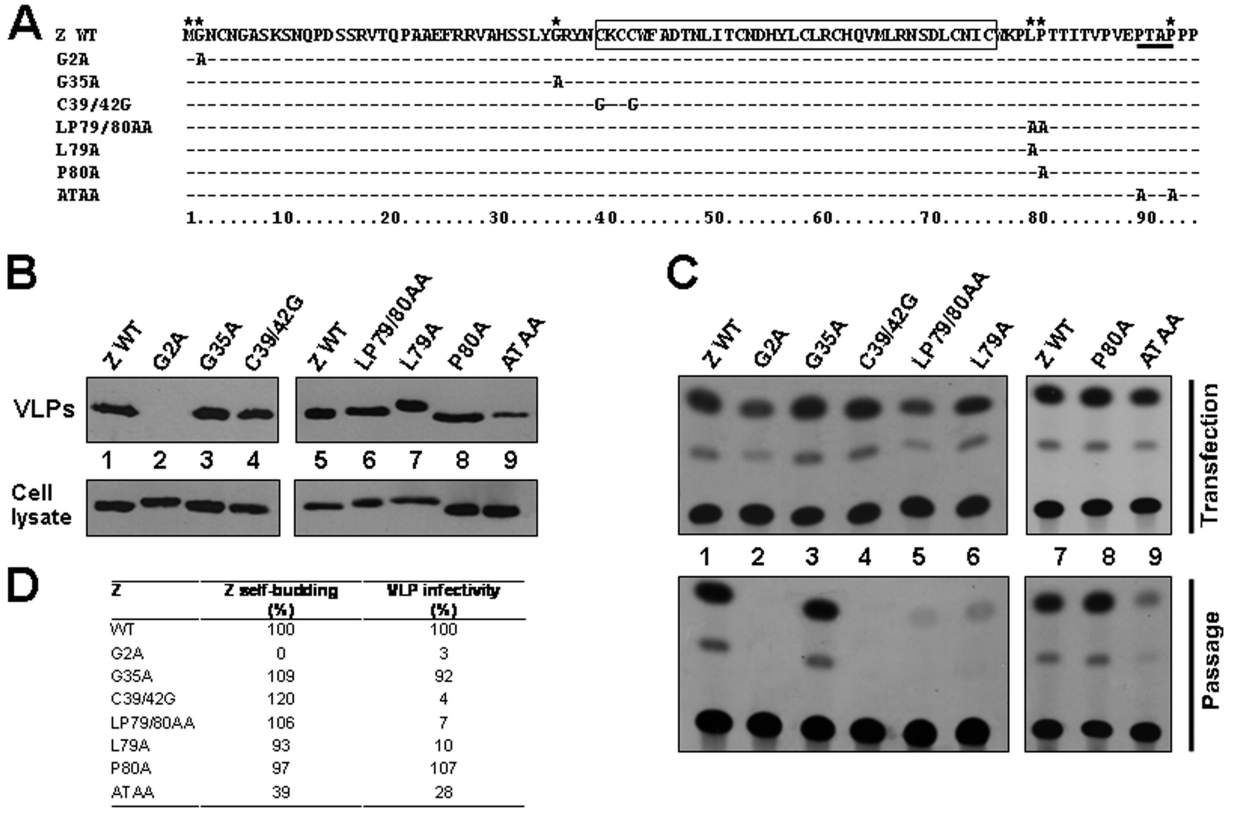

D

Z	Z self-budding (%)	VLP infectivity (%)
WT	100	100
G2A	0	3
G35A	109	92
C39/42G	120	4
LP79/80AA	106	7
L79A	93	10
P80A	97	107
ATAA	39	28

FIG. 4. (A) JunV WT and mutant Z proteins. The amino acid sequence of Z WT is shown on top. Amino acids within the RING domain are indicated by an empty box. The PTAP motif is underlined. Residues strictly conserved outside the RING domain in all sequenced arenavirus Z proteins are indicated by stars. Z mutant sequences are below, the substitutions are shown at the corresponding positions, and unmodified residues are indicated by dashes. The C-terminal HA epitope sequence was omitted from both WT and mutant Z proteins. (B) Z self-budding. BSR cells grown in 12-well plates were transfected with 0.5 μg of either pJunV Z-HA (Z WT) (lanes 1 and 5) or each of the Z mutant-expressing plasmids as indicated (lanes 2 to 4 and 6 to 9). Aliquots of both cell extracts and purified VLPs were analyzed by Western blotting (Materials and Methods). It should be noticed that the slightly retarded electrophoretic mobility observed for mutants G2A, LP79/80AA, and L79A (lanes 2, 6 and 7) was consistently observed among all the experiments. Results shown in lanes 1 to 4 and lanes 5 to 9 correspond to two independent experiments. (C) Infectivity of VLPs. BSR cells were transfected with plasmids expressing S-CAT minigenome, TacV L, TacV N, and JunV GP together with either pJunV Z-HA (Z WT) (lanes 1 and 7) or each of the Z mutant-expressing plasmids as indicated (lanes 2 to 6 and 8 and 9) at the amounts used in the experiments shown in Fig. 1 and 2. The corresponding supernatants were collected, and cell extracts were prepared for determination of CAT activity (Transfection), as indicated in Materials and Methods. Clarified culture supernatants were added to CV1 cell monolayers, which were then assayed for CAT activity (Passage). Quantification of CAT activity was performed as indicated in Materials and Methods. Results shown in lanes 1 to 6 and lanes 7 to 9 correspond to two independent experiments. (D) Z self-budding corresponds to the ratio between Z protein detected in VLPs and total (VLP plus cellular) Z protein. The amount of Z in cell extracts was normalized for β-tubulin as indicated in Materials and Methods. VLP infectivity was calculated as CAT activity in Passage normalized for CAT activity in Transfection. Values correspond to the mean from at least three independent experiments and are expressed as the percentage of Z WT, set as 100%. Standard deviations ranged from 0% (G2A) to 21% (ATAA) for Z self-budding and from 2% (G2A) to 20% (P80A) for VLP infectivity.

(lanes 1 and 2), suggesting that Z and N interact with each other within VLPs in the absence of the minigenome and other viral proteins.

Effect of the mutations in Z protein on Z release and VLP infectivity. Comparison of the currently available deduced protein sequences of all arenavirus Z genes reveals a similar organization, with a central RING domain surrounded by less conserved N- and C-terminal regions. In order to identify amino acids in Z relevant for VLP infectivity, we modified residues in the JunV Z protein that are strictly conserved among all known arenavirus Z proteins. We replaced the glycine residue at position 35 within the N-terminal region, as well as both L79 and P80 within the C-terminal region, with alanine (Fig. 4A). To disrupt the folding and function of the RING domain (3), we also replaced residues C39 and C42 with glycines, obtaining mutant C39/42G (Fig. 4A). To validate the analysis, Z mutants predicted to display reduced or impaired budding activities were generated. For this, we introduced alanine substitutions in the proline residues of the canonical PTAP motif of JunV Z, obtaining the mutant ATAA. In addition, we replaced the strictly conserved glycine at position 2 with alanine, generating the mutant G2A (Fig. 4A). It has been shown that this modification abolishes LFV and LCMV Z protein myristoylation, the association of Z with the plasma membrane, and Z-mediated budding (36, 45).

To test the ability of Z mutants to display self-budding, either wild-type JunV Z-HA (hereafter, Z WT) or each of the Z mutants containing a C-terminal HA tag was individually expressed in BSR cells, and aliquots of both cell lysates and VLPs were analyzed by Western blotting followed by densito-

metric quantification of the bands. The results showed equivalent expression of all Z mutants in the cell lysates (Fig. 4B, bottom panels). As predicted, the amounts of Z released from the cells expressing the mutant G2A or the mutant ATAA were undetectable (for G2A) or markedly lower (for ATAA) than those released from Z WT-expressing cells (Fig. 4B, lanes 2 and 9, and D). In contrast, nearly WT levels of Z were released from cells expressing either G35A or LP79/80AA mutant or from cells expressing the single point mutants L79A or P80A (Fig. 4B, compare lane 3 to lane 1 and lanes 6, 7, and 8 to 5, and D), showing that residue G35, L79, or P80 is not critically involved in Z self-budding. In addition, the observation that the replacement of both residues C39 and C42 with glycine (Z mutant C39/42G) had no adverse effect on the amount of Z released indicated that the integrity of the RING domain is not strictly required for the efficient release of Z-containing particles (Fig. 4B, compare lanes 4 and 1, and D).

We then evaluated the ability of the Z mutants to form infectious VLPs. To this end, the supernatants collected from BSR cells transfected with the complete set of plasmids, including either pJunV Z-HA or each of the Z mutant-expressing plasmids, were used to inoculate CV1 cells, which were then monitored for passage of S-CAT minigenome (Fig. 4C, Passage). VLP-producing BSR cells were also tested for CAT expression (Fig. 4C, Transfection). The comparison between VLP infectivity, assessed as indicated in the figure legend, and the self-budding ability of each mutant is shown in Fig. 4D. It can be seen, as expected, that the abilities of mutants ATAA and G2A to direct the production of infectious VLPs correlated with their limited self-budding capacities. Among all the mutants showing nearly WT levels of self-budding (G35A, C39/42G, LP79/80AA, L79A, and P80A), only mutants G35A and P80A displayed WT ability to form infectious VLPs, whereas mutants C39/42G and LP79/80AA as well as L79A exhibited a dramatic reduction in ability to direct CAT activity passage (Fig. 4C and D). These results demonstrated that disruption of the RING structure or the replacement of L79 with alanine dramatically impairs the infectivity of VLPs without modifying the self-budding property of Z.

Disruption of the RING structure or mutation of residue L79 of Z severely impairs intracellular Z-N interactions and the incorporation of N into VLPs. As the above results demonstrated that Z protein is sufficient to drive the incorporation of N protein into Z-induced particles (Fig. 3), we analyzed the ability of the Z mutants to recruit N protein into budding particles in the absence of other viral components. To this end, either Z WT or each of the Z mutants displaying impaired abilities to generate infectious VLPs or mutant P80A as control was coexpressed with N, and the released VLPs were purified and analyzed by Western blotting. The results confirmed that, upon coexpression with Z WT, N is recruited into Z-directed VLPs (Fig. 5A, lane 1). Likewise, coexpression of N and the mutant P80A resulted in the release of N into the supernatant (lane 5). In contrast, mutants C39/42G, L79A, and LP79/80AA failed to recruit N into the released particles (VLPs, lanes 2, 3 and 4) even though similar expression levels of both N and Z proteins were detected under all transfection conditions (Fig. 5A, Cell lysate, lanes 1 to 5). Thus, disruption of the RING structure or mutation of L79 to alanine abolishes the ability of Z to mediate the incorporation of N into VLPs.

To further investigate the effect of L79A and C39/42G mutations on the association between Z and N, we first examined the intracellular localization of N and either Z WT or each mutant Z protein by confocal microscopy (Materials and Methods). Figure 5B shows that, when expressed individually, the N protein exhibited diffuse staining and presented discrete structures of various sizes all over the cytoplasm (frame A). Z mutants appeared similar in distribution to Z WT, mostly localizing at the plasma membrane and in discrete structures throughout the cytoplasm (compare frames C and D with B). Coexpression with N did not affect the distribution of Z WT or Z mutants compared with single expression of these proteins (Fig. 5B, compare frames E, H, and K with B, C, and D, respectively). On the other hand, upon coexpression of N with Z WT, a fraction of N was localized at the plasma membrane (compare frames F and A), where N and Z WT appeared to colocalize (frame G). However, when either the C39/42G or L79A mutant was coexpressed with N, no major changes in the subcellular distribution of N compared to cells expressing N alone were evident (compare frames I and L with A), and no plasma membrane localization of N was observed (frames J and M). These phenotypes were present in >90% of the analyzed cells. Similar results were observed when transfections were performed into CHO cells (data not shown), supporting the notion that residue L79 and the RING structure within Z may be involved in direct Z-N interactions.

To further substantiate these results, we analyzed Z-N interactions by means of a coimmunoprecipitation assay. Briefly, CV1 cells coexpressing TacV N-myc and either Z WT or each of the Z mutants (C39/42G or L79A) were metabolically labeled, and aliquots of the cell lysates were immunoprecipitated with specific serum to detect N or Z, followed by SDS-PAGE (Materials and Methods). As a control, a similar procedure was performed with extracts from cells expressing N-myc or Z WT alone (Fig. 5C). Coimmunoprecipitation analyses using anti-HA antibody showed that upon coexpression with N, each of the Z mutants was synthesized at levels similar to WT Z (compare lanes 3 and 4 to lane 2). In addition, coimmunoprecipitation of N and Z WT was observed (lane 2). The specificity of the interaction was demonstrated by the fact that no N was detected when extracts from cells expressing comparable amounts of N alone were analyzed (lane 5). Results also indicated that mutants C39/42G and L79A (lanes 3 and 4) displayed a reduced ability to interact with N compared to that of Z WT (lane 2). This observation was confirmed by immunoprecipitation with serum against c-Myc. Quantification of the results showed that mutants C39/42G and L79A each exhibited binding abilities to N of no more than 40% compared to the binding ability of Z WT.

Overall, these results demonstrated that the disruption of the RING structure or the mutation of residue L79 to alanine within Z drastically affects both intracellular Z-N interactions and the ability of Z to direct the incorporation of N into VLPs.

It is noteworthy that in previous reports we provided the first evidence that Z, at expression levels producing inhibition of viral transcription and replication, interacted with L but not with N. In those studies 50 to 150 ng of Z-expressing plasmids was used (21, 48). At higher levels (about 10-fold) of either the JunV Z-expressing plasmid (present report) or the plasmid expressing TacV Z (M. Wilda, unpublished data), Z-N interactions were readily detected.

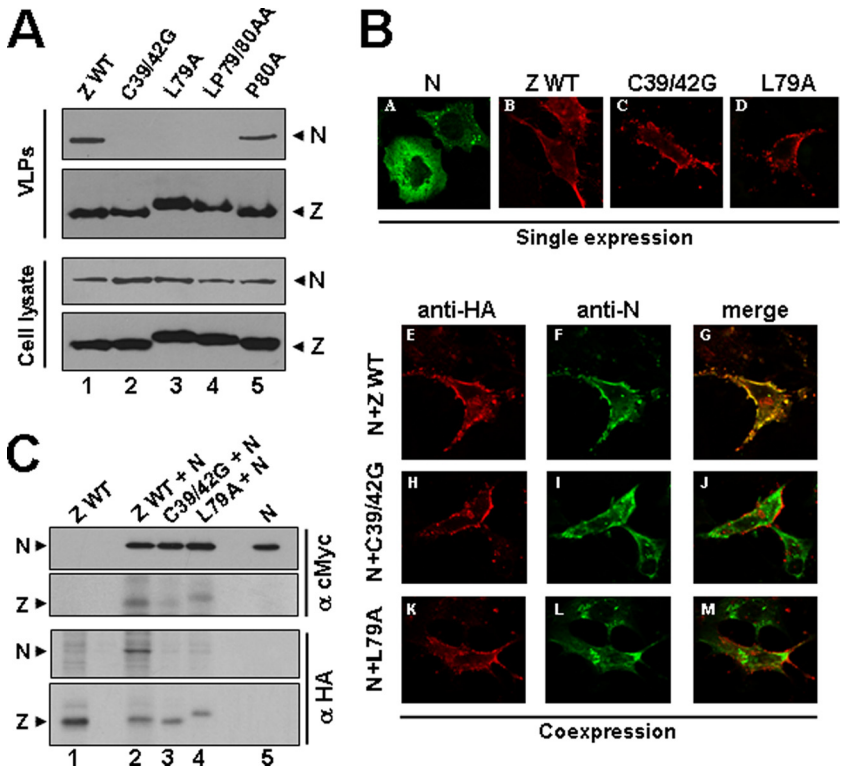

FIG. 5. (A) Recruitment of N into Z-containing VLPs. BSR cells grown in 12-well plates were transfected with 1.5 μg of pTacV N-Flag together with 0.5 μg of either pJunV Z-HA (Z WT) (lane 1) or each of the Z mutant-expressing plasmids, as indicated (lanes 2 to 5). Cell lysates and VLPs were prepared as indicated in Materials and Methods. Samples of both VLPs and cell lysates were analyzed by Western blotting using either anti-Flag or anti-HA antibodies. The positions of N-Flag (N) and Z-HA (Z) proteins are indicated by arrowheads. (B) Intracellular distribution of N and Z proteins. BSR cells expressing individually either N (frame A), Z WT (frame B) or Z mutants (frames C and D) or coexpressing N with either Z WT (frames E to G) or each Z mutant (frames H to M) as shown were fixed, permeabilized and then probed with a mouse anti-TacV N (green) and a rabbit anti-HA antibody (red), as indicated in Materials and Methods. Frames G, J, and M show merged images of the signals for N and Z proteins, as indicated. (C) Coimmunoprecipitation analysis. Cells coexpressing TacV N-myc and either Z WT or each of the Z mutants as indicated (lanes 2 to 4) or expressing either Z WT (lane 1) or TacV N-myc (lane 5) alone were radioactively labeled as indicated in Materials and Methods. Aliquots of the cell lysates were immunoprecipitated using serum against either c-Myc (panel α cMyc) or HA (panel α HA), and the immunoprecipitated proteins were resolved and visualized as described in Materials and Methods. The positions of Z-HA (Z) and N-myc (N) are indicated by arrowheads. In lane 5, the amount of transfected pTacV N-myc plasmid DNA was adjusted (Materials and Methods) such that equivalent amounts of N-myc protein relative to lanes 2 to 4 were expressed. α, anti.

Z-N interactions are required for the assembly of GP into VLPs. To assess whether the Z mutants C39/42G and L79A were able to recruit GP into budding particles, cells were cotransfected with pTacV N and pJunV GP together with either pJunV Z-HA or each of the Z mutant-expressing plasmids. Control cultures in which either the N-, GP-, or Z WT-expressing plasmid was omitted were also included in these experiments (Fig. 6). Transfected cells were metabolically labeled, cell extracts were prepared, and culture supernatants were ultracentrifuged for VLP purification (Materials and Methods). Aliquots of both purified VLPs and cell lysates were analyzed by SDS-PAGE after immunoprecipitation with specific serum to detect either JunV Z-HA, N, or G1 protein. The results revealed that in addition to N and Z proteins, G1 was released into the supernatants of cells coexpressing TacV N, JunV GP, and Z WT (Fig. 6, VLPs, lane 4). The data also indicated that these VLPs displayed G1-to-Z ratios about 7- to 14-fold higher than those in VLPs released from cells coexpressing GP and Z WT in the absence of N (compare lanes 4 and 1 of the VLP panel). These results confirmed our findings (Fig. 2) that coexpression with N enhances the incorporation of GP into WT Z-directed VLPs and revealed that neither the L protein nor the minigenome was required for the assembly of GP into VLPs. Results also showed that coexpression of either the C39/42G or L79A mutant with GP and N resulted in the release of VLPs which displayed no N and in which nearly WT levels of mutant Z protein along with background amounts of G1 were detected (VLPs, lanes 5 and 6). Intracellular levels of N and G1 in Z mutant-expressing cells were similar to those detected in cells expressing Z WT (Cell lysate, compare lanes 5 and 6 with lane 4), showing that these results were not due to a different intracellular accumulation of N or GP. Thus, Z mutants L79A and C39/42G, which display impaired abilities to interact with N (Fig. 5), direct a strongly diminished incorporation of G1 into VLPs.

DISCUSSION

We have established here a transfection-based system for generating arenavirus VLPs. In this system, TacV-like nucleo-

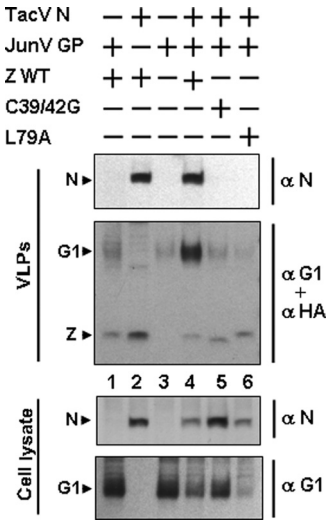

FIG. 6. Effect of mutations in the Z protein on the assembly of GP into VLPs. BSR cells were transfected with plasmids expressing TacV N, JunV GP, and either Z WT or each of the Z mutants, as indicated, at the amounts used for the experiments shown in Fig. 1 and 2. Cells were metabolically labeled, and aliquots of both cell lysate and purified VLPs were immunoprecipitated with antibodies against JunV G1 (α G1) or TacV N (α N) or with a mixture of anti-JunV G1 and anti-HA antibodies (α G1+α HA). Precipitated polypeptides were resolved by SDS-PAGE, visualized by autoradiography, and quantified, as indicated in Materials and Methods. The positions of N, G1, and Z-HA (Z) are indicated by arrowheads. α, anti.

capsids were assembled into VLPs together with Z and GP of the closely related JunV. These VLPs are infectious and can be neutralized by specific anti-JunV antibodies (Fig. 1), indicating that key molecular interactions between the coexpressed TacV and JunV proteins are conserved. This is consistent with previous studies showing that LFV Z can substitute for LCMV Z in formation of infectious VLPs and that LFV GP can replace LCMV GP in generation of a recombinant LCMV variant (37, 39).

The failure of TacV Z to mediate detectable minigenome passage (Fig. 1A) could be attributed to the strong inhibition displayed by TacV Z on reporter gene expression. Notably, cells expressing TacV Z and TacV GP along with N and L proteins displayed about 10-fold lower levels of reporter gene expression than cells coexpressing comparable amounts of JunV Z and JunV GP (Fig. 1A, Transfection). Thus, a lower intracellular accumulation of encapsidated minigenome to be assembled into VLPs could explain the undetectable transfer of CAT activity to new cells. Additionally, since TacV Z does not contain a canonical proline-rich late motif, a lower ability of TacV Z protein to drive VLP formation could also contribute to the observed low levels of TacV Z-mediated minigenome passage.

We also found that, when assembled into complete JunV Z-driven VLPs, TacV GP mediated lower levels of CAT activity passage than JunV GP (Fig. 1A). Taking into account that TacV GP can be incorporated into JunV Z-directed VLPs at levels comparable to those of JunV GP (J. C. Casabona et al., unpublished results), this observation could be attributed to differences in entry efficiencies and/or receptor usage between TacV and JunV GPs (14, 35).

Our results showing that JunV Z displays self-budding, that the omission of JunV Z protein prevents the production of VLPs (Fig. 2 and 3), and that Z-mediated budding is severely affected by the mutation of either the myristoylation site or the PTAP late motif of Z (Fig. 4) are consistent with previous reports on LFV and LCMV (36, 37, 45, 46), further supporting the notion that Z is the driving force for arenavirus particle release.

Direct interaction between the nucleoprotein and the matrix protein has been associated with the incorporation of nucleocapsid-like structures into matrix protein-driven VLPs of other negative-stranded RNA viruses such as human parainfluenza type 1 and Ebola viruses (10, 24, 34). Similarly, our finding that Z protein in the absence of minigenome and other viral proteins was sufficient to recruit N within lipid-enveloped Z-containing VLPs (Fig. 3) supported the idea that Z-N interactions could facilitate the packaging of nucleocapsids into VLPs. To address this point, we generated Z mutants carrying substitutions in residues strictly conserved in all arenaviruses and evaluated the ability of Z mutants to drive self-budding, to interact with N in vivo, and to direct the formation of infectious VLPs. We demonstrated that replacing the strictly conserved G35 or P80 with alanine has little or no effect in either Z self-budding or VLP infectivity. By contrast, disruption of the RING structure or mutation of residue L79, although it did not affect Z self-budding, dramatically impaired the ability of Z to direct infectious VLP formation (Fig. 4). Further, these mutations abrogated the capacity of Z to recruit N into Z-containing VLPs and severely affected intracellular Z-N interactions, as evidenced by coimmunoprecipitation analyses. Consistent with these results, confocal microscopy suggested that the RING structure and residue L79 of Z are required for N localization at the plasma membrane (Fig. 5). We also examined the requirement of different viral components for the incorporation of GP into budding particles. We demonstrated that coexpression of TacV N highly increased the levels of GP incorporated into VLPs (Fig. 2), a result that was reproduced when both S-CAT minigenome and L protein were omitted (Fig. 6) and also when JunV GP was replaced with TacV GP in the system (data not shown). More important, residue L79 and the integrity of the RING structure of Z are necessary for the assembly of GP into VLPs (Fig. 6). Taken together, these results showed that the RING structure and residue L79 of Z are critically important for its binding to N and led us to propose a model in which Z-N interactions govern the localization of viral nucleocapsids to the sites of budding at the plasma membrane, contributing to their subsequent packaging into viral particles. In addition, the data support the suggestion that interactions between GP and Z-N complexes may be involved in the efficient incorporation of GP into infectious virions. Based on recent evidence showing that Z and GP from both LCMV and LFV interact in vivo, it has been speculated that the Z-GP association might contribute to arenavirus particle assembly (6) in a similar way that the matrix protein-glycoprotein interactions are important for glycoprotein incorporation in other virus systems such as human immunodeficiency virus type 1, rabies, and Marburg viruses (11, 17, 29, 30). Considering that the integrity of the Z RING domain is not required for either LCMV or LFV Z-GP interactions (6), our results suggest that

Z might have different GP-binding properties when complexed with N during particle assembly.

It is unclear whether residue L79 and the RING structure are both involved in direct interactions between N and Z. However, as destabilization of the first zinc-binding site of the RING structure abolishes the capacity of either LCMV or LFV Z to self-associate in vitro (22), it is also possible that the binding of N at the putative N-binding site of Z could require the RING-dependent oligomerization of Z protein. Current efforts are under way to define further residues of Z and the regions of N that participate in Z-N interactions important for the assembly of viral particles. A better understanding of the molecular determinants involved in the assembly of infectious particles will be helpful for the design of new strategies for controlling pathogenic human arenaviruses.

ACKNOWLEDGMENTS

We are very grateful to María Teresa Franze-Fernández (University of Buenos Aires, Argentina) for continuous support, invaluable discussions, and critical reading of the manuscript. We thank especially Osvaldo Rey (University of Los Angeles, CA), Maximiliano Wilda (University of Buenos Aires, Argentina), and Natalia Frias-Staheli (Mount Sinai School of Medicine, NY) for helpful discussions and for manuscript reviews. We also thank Martin A. Billeter (University of Zurich, Irchel, Switzerland), Michael Buchmeier (The Scripps Research Institute, La Jolla, CA), Elsa Damonte (University of Buenos Aires, Argentina), Ramon Flick (University of Texas, Galveston, TX), and Bernard Moss (National Institutes of Health, Bethesda, MD) for generously providing reagents. Anti-JunV MAbs were provided by the NIH Biodefense and Emerging Infections Research Resources Repository (National Institute of Allergy and Infectious Diseases, NIH). The technical assistance of J. Acevedo and S. Rojana is acknowledged.

This work was supported by Agencia Nacional de Promoción Científica y Tecnológica and CONICET. N.L. is a research investigator of CONICET. J.C.C., J.M.L.M., M.E.L., and G.A.G. are recipients of a fellowship from this institution.

REFERENCES

1. **Abramoff, M. D., P. J. Magelhaes, and S. J. Ram.** 2004. Image processing with ImageJ. Biophotonics Int. **11:**36–42.
2. **Bishop, D. H. L., and D. D. Auperin.** 1987. Arenavirus gene structure and organization. Curr. Top. Microbiol. Immunol. **133:**5–17.
3. **Borden, K. L. B., E. J. Campbell Dwyer, and M. S. Salvato.** 1998. An arenavirus RING (zinc-binding) protein binds the oncoprotein promyelocyte leukemia protein (PML) and relocates PML nuclear bodies to the cytoplasm. J. Virol. **72:**758–766.
4. **Bowen, M. D., C. J. Peters, and S. T. Nichol.** 1996. The phylogeny of New World (Tacaribe complex) arenaviruses. Virology **219:**285–290.
5. **Buchmeier, M. J., J. C. de la Torre, and C. J. Peters.** 2007. *Arenaviridae*: the viruses and their replication, p. 1791–1828. *In* D. M. Knipe, P. M. Howley, D. E. Griffin, R. A. Lamb, M. A. Martin, B. Roizman, and S. E. Straus (ed.), Fields virology, 5th ed. Lippincott Williams & Wilkins, Philadelphia, PA.
6. **Capul, A. A., M. Perez, E. Burke, S. Kunz, M. J. Buchmeier, and J. C. de la Torre.** 2007. Arenavirus Z-glycoprotein association requires Z myristoylation but not functional RING or late domains. J. Virol. **81:**9451–9460.
7. **Charrel R. N., X. de Lamballerie, and S. Emonet.** 2008. Phylogeny of the genus *Arenavirus*. Curr. Opin. Microbiol. **11:**362–368.
8. **Cornu, T. I., H. Feldmann, and J. C. de la Torre.** 2004. Cells expressing the RING finger Z protein are resistant to arenavirus infection. J. Virol. **78:** 2979–2983.
9. **Cornu, T. I., and J. C. de la Torre.** 2001. RING finger Z protein of lymphocytic choriomeningitis virus (LCMV) inhibits transcription and RNA replication of an LCMV S-segment minigenome. J. Virol. **75:**9415–9426.
10. **Coronel, E. C., K. Gopal Murti, T. Takimoto, and A. Portner.** 1999. Human parainfluenza virus type 1 matrix and nucleoprotein genes transiently expressed in mammalian cells induce the release of virus-like particles containing nucleocapsid-like structures. J. Virol. **73:**7035–7038.
11. **Cosson, P.** 1996. Direct interaction between the envelope and matrix proteins of HIV-1. EMBO J. **15:**5783–5788.
12. **Eichler, R., T. Strecker, L. Kolesnikova, J. ter Meulen, W. Weissenhorn, S. Becker, H. D. Klenk, W. Garten, and O. Lenz.** 2004. Characterization of the Lassa virus matrix protein Z: electron microscopic study of virus-like particles and interaction with the nucleoprotein (NP). Virus Res. **100:**249–255.
13. **Enria, D. A., A. M. Briggiler, and Z. Sanchez.** 2008. Treatment of Argentine hemorrhagic fever. Antivir. Res. **78:**132–139.
14. **Flanagan, M. L., J. Oldenburg, T. Reignier, N. Holt, G. A. Hamilton, V. K. Martin, and P. M. Cannon.** 2008. New World clade B arenaviruses can use transferrin receptor 1 (TfR1)-dependent and -independent entry pathways, and glycoproteins from human pathogenic strains are associated with the use of TfR1. J. Virol. **82:**938–948.
15. **Flick, R., and R. F. Pettersson.** 2001. Reverse genetics system for Uukuniemi virus (*Bunyaviridae*): RNA polymerase I-catalyzed expression of chimeric viral RNAs. J. Virol. **75:**1643–1655.
16. **Franze-Fernández, M. T., S. Iapalucci, N. López, and C. Rossi.** 1993. Subgenomic RNAs of Tacaribe virus, p. 113–132. *In* M. S. Salvato (ed.), The *Arenaviridae*. Plenum Press, New York, NY.
17. **Freed, E. O., and M. A. Martin.** 1996. Domains of the human immunodeficiency virus type 1 matrix and gp41 cytoplasmic tail required for envelope incorporation into virions. J. Virol. **70:**341–351.
18. **Fuerst, T. R., E. G. Niles, F. W. Studier, and B. Moss.** 1986. Eukaryotic transient-expression system based on recombinant vaccinia virus that synthesizes bacteriophage T7 RNA polymerase. Proc. Natl. Acad. Sci. USA **83:**8122–8126.
19. **Howard, C. R., H. Lewicki, L. Allison, M. Salter, and M. J. Buchmeier.** 1985. Properties and characterization of monoclonal antibodies to Tacaribe virus. J. Gen. Virol. **66:**1383–1395.
20. **Iglesias-Bartolomé, R., P. M. Crespo, G. A. Gómez, and J. L. Daniotti.** 2006. The antibody to GD3 ganglioside, R24, is rapidly endocytosed and recycled to the plasma membrane via the endocytic recycling compartment. Inhibitory effect of brefeldin A and monensin. FEBS J. **273:**1744–1758.
21. **Jácamo, R., N. López, M. Wilda, and M. T. Franze-Fernández.** 2003. Tacaribe virus Z protein interacts with the L polymerase protein to inhibit viral RNA synthesis. J. Virol. **77:**10383–10393.
22. **Kentsis, A., R. E. Gordon, and K. L. B. Borden.** 2002. Self-assembly properties of a model RING domain. Proc. Natl. Acad. Sci. USA **99:**667–672.
23. **Kolakofsky, D., and D. Garcin.** 1993. The unusual mechanism of arenavirus RNA synthesis p. 103–112. *In* M. S. Salvato (ed.), The *Arenaviridae*. Plenum Press, New York, NY.
24. **Licata, J. M., R. F. Johnson, Z. Han, and R. N. Harty.** 2004. Contribution of Ebola virus glycoprotein, nucleoprotein, and VP24 to budding of VP40 virus-like particles. J. Virol. **78:**7344–7351.
25. **López, N., L. Scolaro, C. Rossi, R. Jácamo, N. Candurra, C. Pujol, E. B. Damonte, and M. T. Franze-Fernandez.** 2000. Homologous and heterologous glycoproteins induce protection against Junin virus challenge in guinea pigs. J. Gen. Virol. **81:**1273–1281.
26. **López, N., and M. T. Franze-Fernández.** 2007. A single stem-loop structure in Tacaribe arenavirus intergenic region is essential for transcription termination but is not required for a correct initiation of transcription and replication. Virus Res. **124:**237–244.
27. **López, N., R. Jácamo, and M. T. Franze-Fernández.** 2001. Transcription and RNA replication of Tacaribe virus genome and antigenome analogs require N and L proteins: Z protein is an inhibitor of these processes. J. Virol. **75:**12241–12251.
28. **Martínez-Peralta, L. A., C. E. Coto, and M. C. Weissenbacher.** 1993. The Tacaribe complex: the close relationship between a pathogenic (Junin) and a nonpathogenic (Tacaribe) arenavirus, p. 281–296. *In* M. S. Salvato (ed.), The *Arenaviridae*. Plenum Press, New York, NY.
29. **Mebatsion, T., F. Weiland, and K. K. Conzelmann.** 1999. Matrix protein of rabies virus is responsible for the assembly and budding of bullet-shaped particles and interacts with the transmembrane spike glycoprotein G. J. Virol. **73:**242–250.
30. **Mittler, E., L. Kolesnikova, T. Strecker, W. Garten, and S. Becker.** 2007. Role of the transmembrane domain of Marburg virus surface protein GP in assembly of the viral envelope. J. Virol. **81:**3942–3948.
31. **Morita, E., and W. I. Sundquist.** 2004. Retrovirus budding. Annu. Rev. Cell Dev. Biol. **20:**395–425.
32. **Moss, B., O. Elroy-Stein, T. Mizukami, W. A. Alexander, and T. R. Fuerst.** 1990. Product review. New mammalian expression vectors. Nature **348:**91–92.
33. **Neuman, B. W., B. D. Adair, J. W. Burns, R. A. Milligan, M. J. Buchmeier, and M. Yeager.** 2005. Complementarity in the supramolecular design of arenaviruses and retroviruses revealed by electron cryomicroscopy and image analysis. J. Virol. **79:**3822–3830.
34. **Noda, T., H. Ebihara, Y. Muramoto, K. Fujii, A. Takada, H. Sagara, J. H. Kim, H. Kida, H. Feldmann, and Y. Kawaoka.** 2006. Assembly and budding of Ebolavirus. PLoS Pathog. **2:**e99.
35. **Oldenburg, J., T. Reignier, M. L. Flanagan, G. A. Hamilton, and P. M. Cannon.** 2007. Differences in tropism and pH dependence for glycoproteins from the clade B1 arenaviruses: implications for receptor usage and pathogenicity. Virology **364:**132–139.
36. **Perez, M., D. L. Greenwald, and J. C. de la Torre.** 2004. Myristoylation of the RING finger Z protein is essential for arenavirus budding. J. Virol. **78:** 11443–11448.
37. **Perez, M., R. C. Craven, and J. C. de la Torre.** 2003. The small RING finger

protein Z drives arenavirus budding: implications for antiviral strategies. Proc. Natl. Acad. Sci. USA **100:**12978–12983.

38. **Radecke, F., P. Spielhofer, H. Schneider, K. Kaelin, M. Huber, C. Dotsch, G. Christiansen, and M. A. Billeter.** 1995. Rescue of measles viruses from cloned DNA. EMBO J. **14:**5773–5784.
39. **Rojek, J. M., A. B. Sanchez, N. T. Nguyen, J. C. de la Torre, and S. Kunz.** 2008. Different mechanisms of cell entry by human-pathogenic Old World and New World arenaviruses. J. Virol. **82:**7677–7687.
40. **Rossi, C., O. Rey, P. Jenik, and M. T. Franze-Fernández.** 1996. Immunological identification of Tacaribe virus proteins. Res. Virol. **147:**203–211.
41. **Salvato, M. S.** 1993. Molecular biology of the prototype arenavirus, lymphocytic choriomeningitis virus, p 133–156. *In* M. S. Salvato (ed.), The *Arenaviridae*. Plenum Press, New York, NY.
42. **Salvato, M. S., K. J. Schweighofer, J. Burns, and E. M. Shimomaye.** 1992. Biochemical and immunological evidence that the 11 kDa zinc-binding protein of lymphocytic choriomeningitis virus is a structural component of the virus. Virus Res. **22:**185–198.
43. **Sanchez, A., D. Y. Pifat, R. H. Kenyon, C. J. Peters, J. B. McCormick, and M. P. Kiley.** 1989. Junin virus monoclonal antibodies: characterization and cross-reactivity with other arenaviruses. J. Gen. Virol. **70:**1125–1132.
44. **Schmitt, A. P., and R. A. Lamb.** 2004. Escaping from the cell: assembly and budding of negative-strand RNA viruses. Curr. Top. Microbiol. Immunol. **283:**145–196.
45. **Strecker, T., A. Maisa, S. Daffis, R. Eichler, O. Lenz, and W. Garten.** 2006. The role of myristoylation in the membrane association of the Lassa virus matrix protein Z. Virol. J. **3:**93.
46. **Strecker, T., R. Eichler, J. Meulen, W. Weissenhorn, H. Dieter Klenk, W. Garten, and O. Lenz.** 2003. Lassa virus Z protein is a matrix protein sufficient for the release of virus-like particles. J. Virol. **77:**10700–10705.
47. **Urata, S., T. Noda, Y. Kawaoka, H. Yokosawa, and J. Yasuda.** 2006. Cellular factors required for Lassa virus budding. J. Virol. **80:**4191–4195.
48. **Wilda, M., N. López, J. C. Casabona, and M. T. Franze-Fernandez.** 2008. Mapping of the Tacaribe arenavirus Z-protein binding sites on the L protein identified both amino acids within the putative polymerase domain and a region at the N terminus of L that are critically involved in binding. J. Virol. **82:**11454–11460.